ASSESSMENT OF MAGNETIC INDUCTION EMISSION GENERATED BY AN UNDERGROUND HV CABLE

Rabah DJEKIDEL[1], Mahi DJILALI[2], Chafik HADJAD[3]

In this work we are interested in numerical calculation of the magnetic flux density in the proximity of a three-phase underground cable circuit in horizontal configuration by the Biot-Savart's law and comparing the levels obtained from the field to the exposure values set by the standards. The results show that these levels are less than the limit recommended by the standards, also this work allows to conclude that the cables in a triangular configuration is the most preferred configuration. The simulation results of magnetic flux density values are compared with those obtained from software COMSOL 3.5a. A good agreement has been obtained.

Keywords: Magnetic flux density, Biot-Savart Law, Three-phase underground cable, Soil effect, COMSOL 3.5a software

1. Introduction

The high voltage electric power transmission network consists of overhead lines, underground cables and substations. Underground insulated cables are mainly used in highly urbanized areas in the suburbs or within the major cities, sometimes to solve environmental technical problems, for which the implementation of overhead transmission lines is difficult or impossible [1,2]. A good management of the transport networks is characterized by an electric service in quantity and quality required by the users, helping to raise the standard of living of the human population, and by producing less possible impact on the environment, in order to respond the concerns of the public opposite the electromagnetic fields generated by this electricity network, in particular the low frequency magnetic fields. The environment has been for about twenty years the subject of social concerns whose exposure to the electromagnetic fields probably constitutes the most important fear expressed by the human population. In general, there is no specific regulation to electromagnetic fields. The International Radiation Protection Association (IRPA) and the International Commission for

[1]Department of Electrical Engineering, Faculty of Technology,University Amar Telidji of Laghouat, Algeria, e-mail: djekidel@mail.lagh-univ.dz
[2] Department of Electrical Engineering, Faculty of Technology,University Amar Telidji of Laghouat, Algeria
[3] Department of Electrical Engineering, Faculty of Technology,University Amar Telidji of Laghouat, Algeria

the Protection against Non-Ionizing Radiation Protection (ICNIRP) recommends an exposure limit, for the general public (residential areas) at 50 Hz is 100 µT for the magnetic flux density. With regard to working environment, this recommendation is 500 µT [3-5]. To achieve this objective, the electric transport companies can study and reduce the values of these fields in the proximity of the limits set by current regulations. In recent years, many articles have been published on the calculation of the magnetic field using analytical and numerical calculations [6-16]. From these previous studies, our task is directed towards a contribution which provides a validation of our results using a modeling with COMSOL 3.5a software package.

In this work, a study of the magnetic flux density generated by an underground cable is presented, Based on the Biot-Savart law and the superposition theorem. Finally, the simulation results will be compared with those determined using COMSOL 3.5a Multiphysics Software based on the finite element method (FEM).

2. Biot-Savart Law

The Biot-Savart Law is one of the most basic laws in magnetostatics, is a superposition method, which describes how the magnetic induction at a given point is produced by moving electric charges at a constant rate (steady current), close to the particular point. In other words, it calculates the magnetic flux density produced at observation point by currents in its proximity [6-9, 17].

Consider a constant current flow through an infinitely long straight conductor (Fig. 1). Using the Biot-Savart law to find the magnetic flux density produced by differential current element $I\vec{dl}$ along the z axis in the xy-plane, as shown in Fig. 1 below.

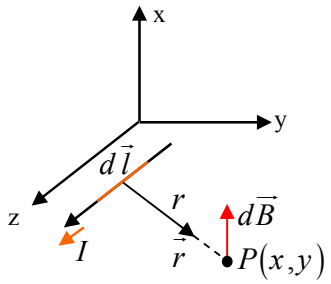

Fig. 1. magnetic flux density dB due to current carrying element

The magnetic flux intensity dB at the observation point P can be written as,

$$d\vec{B} = \frac{\mu_0}{4\pi} \frac{I\,\vec{dl} \times \vec{r}}{r^3} \tag{1}$$

where: I is the magnitude of the current in the direction $\vec{dl}$ tangent to the conductor, r is the distance from the current source to where the magnetic flux density is calculated (point P); $\vec{r}$ is the corresponding unit vector ;μ_0 is the permeability of free space.

Adding up these contributions dB to find the magnetic flux density at the point P requires integrating Equation (1) around the closed circuit C. The total magnetic flux density due to a conductor of infinite length l carrying a current I is [7,8,9]:

$$B = \int_C d\vec{B} = \frac{\mu_0}{4\pi} I \int_{-\infty}^{+\infty} \frac{\vec{r}}{r^3} dl = \frac{\mu_0}{2.\pi} \cdot \frac{I}{r} \tag{2}$$

This relationship shows that the magnetic flux density is directly proportional to the current flowing in the conductor and inversely proportional to the distance of the observation point from the conductor.

3. Underground power cables

The High Voltage electric cables are used when underground electricity transmission is required. These cables are laid in conduits on a hard sole and covered with special sand at low thermal resistance or may be directly buried under the ground. The underground power cable is composed of different parts assembled concentrically, the main ones are: the core conductor to carry current; electrical isolation to prevent current from flowing to the earth, a metal sheath to confine the electric field inside the cable; outdoor protection that provides good mechanical properties and protects against external aggressions [18,19].

Fig. 2 illustrates cross sections of a three-phase cable.

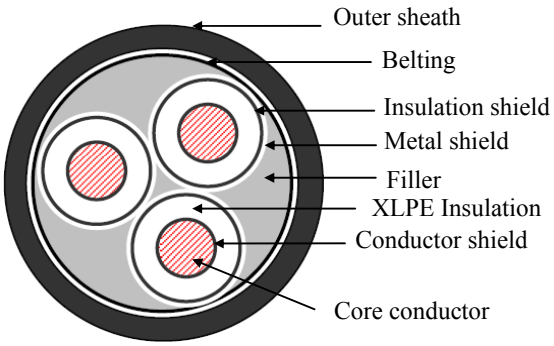

Fig. 2. Cross-section of a three-phase electric cable

4. Magnetic flux density calculation

Fig. 3 shows three-phase electric cable buried in trenches at a depth of yi below ground level and placed, from center to center, at a distance of d from each other. To calculate the magnetic flux density in observation point P due to currents flowing through these conductors, we can use the Biot–Savart law. This calculation considers all conductors constituting the line to be straight, horizontal, of infinite length and parallel to each other, and the effect of the induced shield/sheath currents on the magnetic field is negligible [10-13].

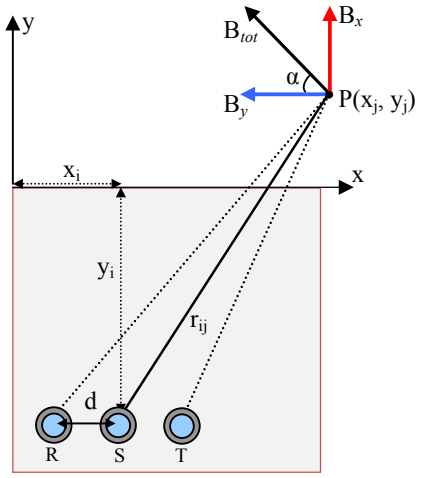

Fig. 3. Calculation of the magnetic flux density generated by a three-phase underground transmission cable

The principle of superposition may be applied to determine the total magnetic field produced by the three-phase electric cable. In the Cartesian coordinate system, according to the Fig. 3,the horizontal and vertical components of magnetic field density at the observation point P due to the current in (n) cable, can be calculated respectively by the formulas given below[11,12].

$$B_{xi} = \sum_{i=1}^{n} -\frac{\mu_0.\mu_r}{2.\pi}.I_i\left[\frac{y_i + y_j}{r_{ij}^{\,2}}\right]$$
$$B_{yi} = \sum_{i=1}^{n} \frac{\mu_0.\mu_r}{2.\pi}.I_i\left[\frac{x_i - x_j}{r_{ij}^{\,2}}\right] \quad (3)$$

Where: x_i and y_i are the coordinates of three-phase conductors; x_j and y_j are the coordinates of observation point P; r is the distance from the current source to point P, is defined as,

$$r_{ij} = \sqrt{\left(x_i - x_j\right)^2 + \left(y_i - y_j\right)^2} \tag{4}$$

The total magnetic flux density produced by the three-phase underground cable at observed point P (x_j, y_j) can be calculated as:

$$B_{tot} = \sqrt{B_{xi}^2 + B_{yi}^2} \tag{5}$$

Calculating the magnetic flux density in case of two adjacent mediums with different relative permeability requires the use of image method. If a current I is placed parallel to a plane surface of high magnetic permeability medium, an image current in the same direction as this current appears, this is because of the boundary condition that the tangential component of the magnetic field should vanish at the surface and this could be done with an image current. That is, there is no tangential component of the field because this is distributed normal to the plane surface and opposite to the current also because of the boundary condition. The image of a current segment perpendicular to the surface is opposite to the current also because of the boundary condition [20,21].

.

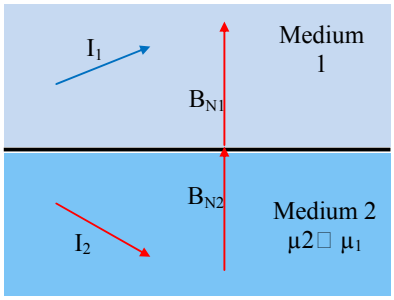

Fig. 4. Image currents I1 in medium 1

If the permeability of the medium is finite, the vector potential in the other region can be calculated by summing contributions from the original current and an image current in air.

$$I_1 = \frac{\mu r_2 - \mu r_1}{\mu r_1 + \mu r_2} I_2 \tag{6}$$

The magnetic flux density B in this region can be determined by assuming an effective current that replaces the original current (For further details, see Ref. 21.).

$$I_2^{'} = I_1 + I_2 = \frac{\mu r_2 - \mu r_1}{\mu r_2 + \mu r_1} I_2 + I_2 = \frac{2.\mu r_2}{\mu r_2 + \mu r_1} . I_2 \tag{7}$$

5. Method validation

In order to validate the proposed method, we can use the COMSOL 3.5a Multiphysics software based on finite element method (FEM), it is a numerical technique used to find solutions of partial differential equations as well as of integral equations to a variety of problems in electromagnetic. COMSOL 3.5a Multiphysics has several tools for all engineering applications, such as electrostatic, magnetostatic, and quasi-static [22-25].

In static analysis, the distribution of the magnetic induction B is derived from the magnetic vector potential A as [22, 26]:

$$\vec{B} = \vec{rot}.\vec{A} \tag{8}$$

When the magnetic vector potential is applied to material medium, where there is not a current density, we get Laplace's equation. In 2D magnetostatic analysis, the resolution of this equation allows to calculate the magnetic induction B produced by the three-phase electric cable, the general form of this equation is [22,26]:

$$\frac{\partial^2 A}{\partial x^2} + \frac{\partial^2 A}{\partial y^2} = 0 \tag{9}$$

This equation is solved by the magnetostatic model using finite element method in COMSOL 3.5a software by applying the boundary conditions at the interface between two different media.

6. Results

To calculate the magnetic-field intensity in this application for 275 kV three-phase electric cable , we consider a three-phase underground cable with XLPE insulation, 2500 mm^2, copper conductor, buried at a depth of 1 m , and placed, from center to center, at a distance of 0.3 m from each other (see Fig. 5). The three cables currents have been assumed under balanced operation with the magnitude of 500A. The soil is considred flat and homogeneous with a constant permeability .Nominal frequency is 50 Hz.

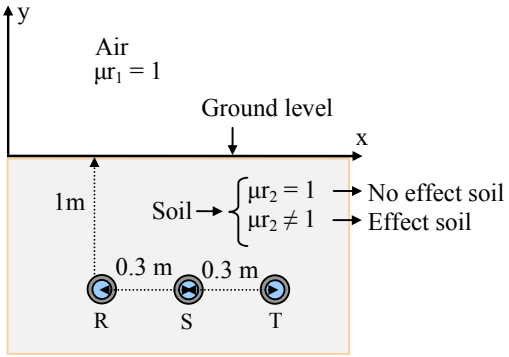

Fig. 5. Three-phase underground transmission cable at a depth of 1 m below ground level

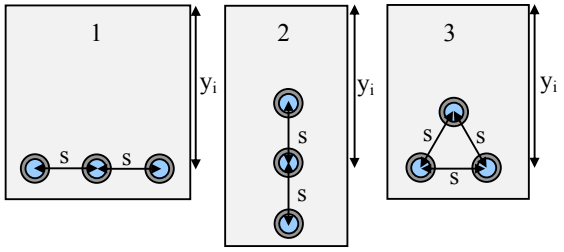

Fig. 6. Different geometrical configurations for three-phase underground transmission cable: (1) horizontal, (2) vertical, (3) triangular

In the first case, it is considered that the soil has no effect on the magnetic flux density, the relative permeability of soil is μr = 1.

Fig. 7 shows the Lateral distribution of the RMS magnetic flux density strength at ground level for the underground power cable, the resultant magnetic flux density peaked B=48.38μT at the cable centerline and decreases rapidly with increasing distance from the cable axis in both directions from the corridor to reach negligible values further away from this center. The maximum value is much lower than the 100 μT recommended value. It appears clear from this figure that the magnetic flux density profile is symmetric about the middle cable.

The variation of the magnetic flux density components in point (x = 0, y = 0) over time is shown in Fig. 8. The graph shows the magnetic flux density created by each cable; this is to say that the magnetic flux density distribution in the cable is not stationary but varies with respect to time. The result allows us to see the relationship between the magnetic flux density strength and the modulus and the direction of the current flowing through the conductor, the higher the current, the greater the strength of the magnetic flux density. We note that the

total magnetic flux density is determined by the superposition of several sinusoidal fields of all cables.

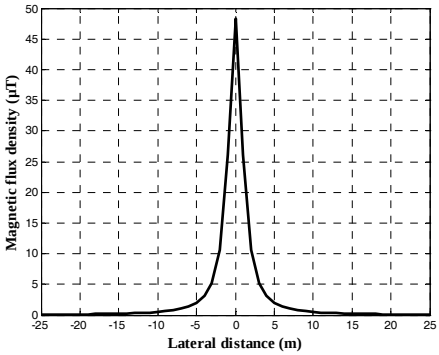

Fig. 7. Magnetic flux density profiles at ground level for the HV Underground Cable for a non magnetic soil ($\mu r = 1$)

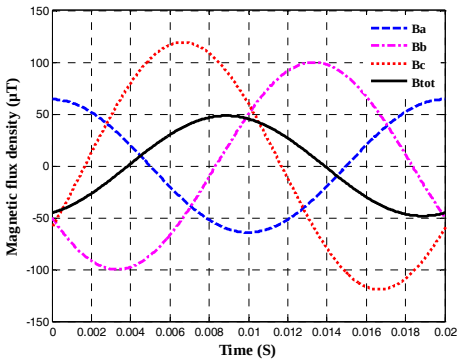

Fig. 8. Three sinusoidal components of the magnetic flux density

The instantaneous variation of both horizontal and vertical components of the vector magnetic flux density (Bx, By) in point (x = 0, y = 0) is shown in Fig. 9. We found the dominance of Horizontal component of the magnetic flux density, the shape curve of this component is virtually superimposed with that of the total magnetic flux density, while the vertical component By is much reduced at ground level, it provides a lesser value of magnetic flux density at this point, this is due to the effect of the calculation point (x = 0, y = 0).

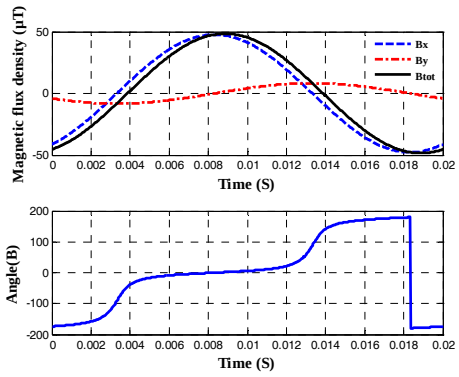

Fig. 9. Temporal variation of modulus and argument of the magnetic flux density

The modulus and the argument of the instantaneous magnetic flux density also are shown in this figure., the peak value of magnetic flux density is obtained at instant t = 0.0089 (s) for argument θ = 1.72 °.

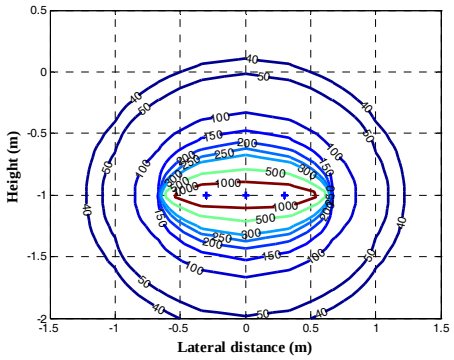

Fig. 10. Contour plots of the magnetic flux density for a three-phase underground power cable

The three contour lines for the magnetic flux density distribution around the underground power cable at any point for the xy-plane are depicted in Fig. 10. The different level of magnetic flux density is due to the variation of coordinates (x, y) of the calculation points from the ground, the intense magnetic flux density lines are in the immediate proximity of the power cables surface.

Fig. 11 describes the mapping of the magnetic flux density of the three-phase HV cable, in an area defined by the vertical coordinate, and the axis of the distance from the underground power cable center. It may be interesting to note that the concentrated level of the magnetic flux density is produced around the

cables; the magnetic flux density gradually decreases with distance from the center of the underground power cable in both directions from the corridor.

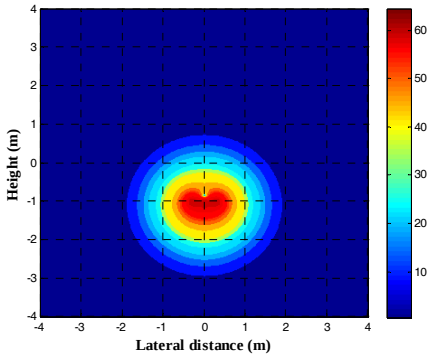

Fig. 11. Mapping of the magnetic flux density generated by a three-phase underground cable

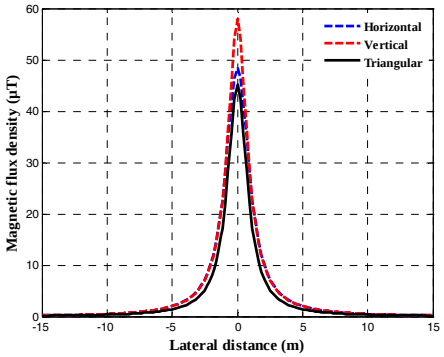

Fig. 12. Lateral profiles of the magnetic flux density at above ground for various phase configurations for a non magnetic soil (μr = 1)

Fig. 12 shows the side profiles of the calculated magnetic flux density at ground level for the three configurations shown in Fig. 6. It appears very clearly that the vertical configuration creates greater magnetic flux density strength with a maximum value of 57.95 μT, whereas the triangular configuration gives lower values for the magnetic flux density magnitude with a maximum of 45.16 μT, hence it can be stated that the triangular configuration is favorable to a reduced magnetic flux density.

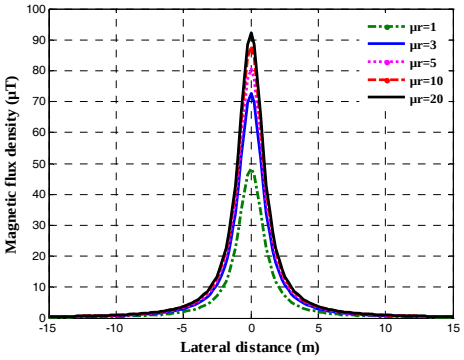

Fig. 13. Magnetic flux density profiles at ground level for the HV Underground Cable for different relative permeability values of the soil.

We note that the maximum magnetic flux density obtained is below the general public exposure level limit; consequently, the standards are met.

In the second case, is considered that the relative permeability of the soil is different to 1 ($\mu r \neq 1$), to reflect the effect of the soil on the magnetic flux density.

Fig. 13 shows the lateral variation of the magnetic induction generated by the electrical cable according to the different values of magnetic permeability of the soil (soil effect). As can be seen, increasing the permeability of the soil increases the values of the magnetic induction at the ground surface.

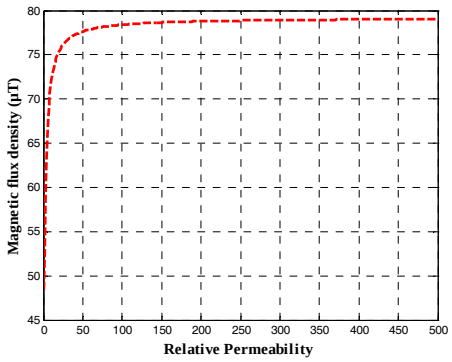

Fig. 14. Profile of the magnetic flux density variation as a function of the relative magnetic permeability of the soil

We can conclude from Fig. 14, that the increase in relative permeability of the soil leading to an increase in magnetic flux density of $\left(2.\ \mu r_2 / \left(\mu r_1 + \ \mu r_2\right)\right)$. With:

μr_1 : is the relative permeability of air $(\mu r_1 = 1)$; μr_2 : is the relative permeability of soil $\mu r_2 \succ 1$.

In order to validate the method adopted in this study, we can use the COMSOL 3.5a Multiphysic software based on the finite element method, the magnetostatic module of this software was used to calculate and analyze the magnetic flux density of the underground power cable, the domain of study presented in Fig. 5 is illustrated by the software COMSOL 3.5a in Fig. 15.

The Visualization of the mesh generated by COMSOL3.5a Multiphysics using linear triangular elements, with the defined settings of the system is shown in Fig. 16.

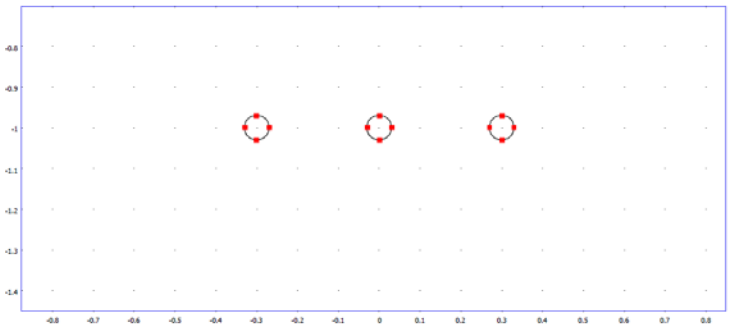

Fig. 15.Illustration of the geometry of the electrical system shown in Fig. 5 using the magnetostatic 2D model in COMSOL 3.5a

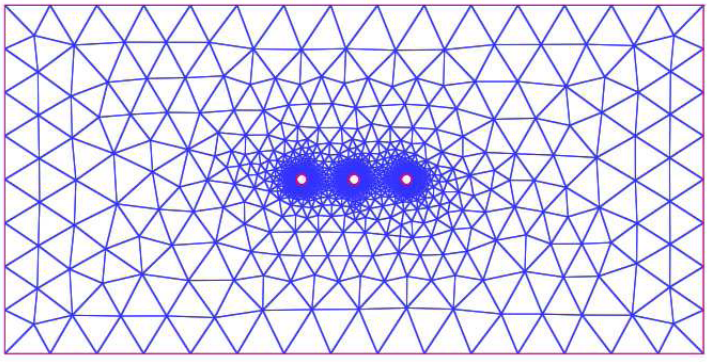

Fig. 16. Discretization of the domain of study given in Fig. 5

Fig. 17 shows the lateral variation of the magnetic flux density strength using the COMSOL 3.5a software for a non magnetic soil (μr = 1). The magnetic flux density takes a maximum value at the center point of the underground cable,

then this field decreases rapidly as one moves away from the center, at a distance of 25 meters, the value is about forty times lower than the maximum value encountered in the proximity of underground power cable.

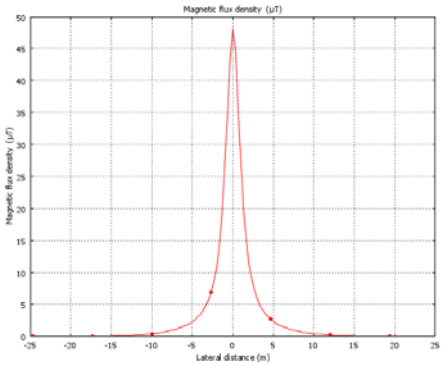

Fig. 17. Lateral distribution of magnetic flux density generate by a three-phase underground cable using COMSOL 3.5a software for a non magnetic soil (μr = 1)

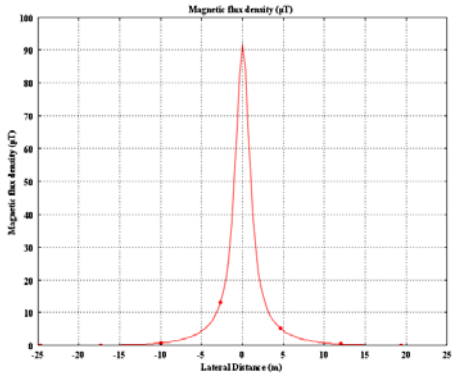

Fig. 18. Lateral distribution of magnetic flux density generate by a three-phase underground cable using COMSOL 3.5a software for a relative magnetic permeability of the soil (μr = 20)

Fig. 18 illustrates the lateral variation of the magnetic flux density strength using the COMSOL 3.5a software for a relative magnetic permeability of the soil equal to 20 (μr = 20). we can see that the maximum value of the magnetic flux density (91.23 μT) is increased compared to that obtained with a relative permeability of soil equal to 1 (47.94 μT).The rate of increase is 1.904.

We have shown in Figs. (19 and 20), the lateral variations of the magnetic flux density obtained by the proposed method, and the simulated values using COMSOL 3.5a software for a non magnetic soil (μr = 1) and for a relative

magnetic permeability of the soil equal to 20 (μr = 20) to consider the effect of soil on the magnetic flux density.

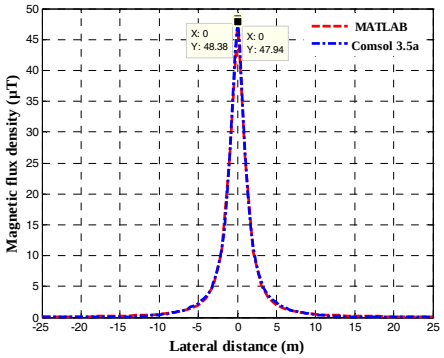

Fig. 19. Comparison of levels of the magnetic flux density between the proposed method and COMSOL 3.5a software for a non magnetic soil (μr = 1)

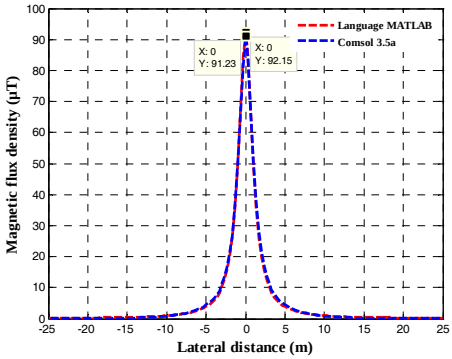

Fig. 20. Comparison of levels of the magnetic flux density between the proposed method and COMSOL 3.5a software for a relative magnetic permeability of the soil (μr = 20)

Comparing the results of these figures, we see a good agreement between the results; the graphs of two figures are perfectly superimposed, this procedure validates and ensures the effectiveness of this method.

7. Conclusion

We used the method of Biot-Savart to quantify and trace the profile of the magnetic flux density under and in the proximity of HV underground cable .We noticed that the value of the magnetic flux density for the configuration chosen in the study is maximum at the center of the underground cable circuit and decreases

with the lateral distance from the middle point of a three-phase cable, we can say that the shape has a symmetrical distribution. For a comparison of different circuit configurations, we can say that the triangular configuration gives a lower magnetic induction than the horizontal and vertical configurations. Maximum values obtained in this simulation are below the values recommended by the standards concerning the environment and the protection of persons. The earth has an effect on the magnetic flux density, the magnetic induction intensity at ground level increases with increasing the relative magnetic permeability of the soil. The obtained results of the magnetic induction of the underground power cable have been compared with simulation results using the COMSOL 3.5a software. The results are close and visually almost identical, the comparison is extremely satisfactory. The proposed method is validated by comparison.

R E F E R E N C E S

[1]. *Michel PAYS,* Câbles de transport d'énergie, Technologies - Caractéristiques, Techniques de l'Ingénieur, traité Génie électrique, D 4520.

[2]. *Ken Dobinson , Rod Bovven ,* Underground Space in the Urban Environment Development and Use, the Warren Centre for Advanced Engineering, The University of Sydney June, 1997.

[3]. *International Commission on Non-Ionizing Radiation Protection*, ICNIRP guidelines for limiting exposure to time - varying electric, magnetic and electromagnetic fields (up to 300 ghz), Health Physics 74 (4):494-522, 1998.

[4]. *J Abstract Book*, International Conference on Electromagnetic Fields from Bioeffects to Legislation, Ljubljana, Slovenia, 2004.

[5]. *Magda Havas*, Biological Effects of Low Frequency Electromagnetic Fields, Electromagnetic Environments and Health in Buildings, London, Chapter 10. 2004

[6]. *Celal Kocatepe, Celal Fadil Kumru ,Eyup Taslak ,* Analysis of magnetic field effects of underground power cables on human health, Proceedings , the 5th International Symposium on Sustainable Development,Turkey , 2014.

[7]. *Keith E. Holbert , George G. Karady , Sanket G. Adhikari , Michael L. Dyer,* Magnetic Fields Produced by Underground Residential Distribution System ,IEEE transactions on power delivery, Vol. 24, No. 3, July. 2009.

[8]. *Jamal M. Ehtaiba ,Sayeh M. Elhabashi*, Magnetic Field Around the New 400kV OH Power Transmission Lines In Libya, Proceedings of the Wseas International Conference on environment, medicine and health sciences, January 2010.

[9]. *Ghanim Thiab Hasan*, Measurements of Electromagnetic Radiations Generated by 11kv Underground Distribution Power Cables, Tikrit Journal of Engineering Sciences, Vol.20/No.3/March 2013.

[10]. *Ahmed S.Farag , Ahmed A.Hossam-eldin , Hanaa M.Karawia,* Magnetic fields management for underground cables structures**,** C I R E D, 21st International Conference on Electricity Distribution Frankfurt, 6-9 June.2011.

[11]. *Earle C. Bascom III, Wayne Banker, Steven A. Boggs, John H. Cooper, Rick Piteo, Angelo M. Regan*, Magnetic Field Management Considerations for Underground Cable Duct Bank, IEEE Transmission & Distribution Conference , New Orleans, Louisiana, 2005.

[12]. *Firoz Ahmad,* Magnetic Field Management in Underground Cables, Master, Thesis of king Fahd University Dahhran, Saudi Arabia.1996.

[13]. *Pedro Miguel Vaz Osório Marchante*, Magnetic field evaluation due to underground power cables, 2009, Instituto Superior Técnico (IST) of the University of Lisbon, Portugal, https://fenix.tecnico.ulisboa.pt.
[14]. *I.O. Habiballah, A.S. Farag, M.M. Dawoud, A. Firoz*, Underground cable magnetic field simulation and management using new design configurations, Electric Power Systems Research, Volume 45, Issue 2, Pages 141–148, May 1998.
[15]. *Budni K, Machczyński W*, Magnetic field of underground cables, the journal Scientific Papers of Silesian University of Technology. Elektryka, volume z 3, 2010.
[16]. *Zairul Aida Abu Zarim Tashia Marie Anthony*, magnetic field simulation & measurement of underground cable system inside duct bank, 22 International Conference on Electricity Distribution Stockholm, Cired, Session 2, Paper No 1089, 10-13 June 2013
[17]. *Mario H Oliveira ,Jose A.Miranda*, Biot-Savart-like law in electrostatics, European Journal of Physics, Theoretical and computational physics Laboratory, Federal University of Pernambuco. Brazil, Volume 22, Number 1 November 2000.
[18]. Nexans. 60-500 kV high voltage underground power cables; XLPE insulated cables. NEXANS France S.A.S - a catalog of a French company active in the cable industry.
[19]. *J R Lucas*, "High Voltage Cables -High Voltage Engineering", 2001.
[20]. Department of Physics & Engineering, Chapter 3, Magnetostatics, University of Saskatchewan, Canada.
[21]. *Kirk T. McDonald*, Dielectric Image Methods Joseph Henry Laboratories, Princeton University, Princeton, NJ 08544, June 10, 2013.
[22]. *Stanley Humphries*, finite-element methods for electromagnetic fields, New Mexico, U.S.A, January 2010,
[23]. *K. Rajagopala, K. Panduranga Vittal, Hemsingh Lunavath*, Computation of Electric Field and Thermal Properties of 3-Phase Cable, Telkomnika, Vol.10, No.2, pp 265-274,June 2012.
[24]. *M Alsharif, P A Wallace, D M Hepburn, C Zhou,* FEM Modeling of Electric Field and Potential Distributions of MV XLPE Cables Containing Void Defect, Excerpt from the Proceedings of the COMSOL Conference in Milan. 2012.
[25]. *R. Djekidel, D. Mahi, A. Ameur, A. Ouchar, M. Hadjadj,* Calcul et atténuation du champ magnétique d'une ligne aérienne HT au moyen d'une boucle passive, ACTA, Electrotehnica Journal, pp 103-108, vol 54, 2013.
[26]. *Young W Kwon , Hyochoong Bang* ,The Finite Elément Method Using MATLAB, , CRC Press Boca Raton London New York Washington, D.C. 1996.